44rd AIAA Aerospace Sciences Meeting and Exhibit, January 912, 2005, Reno, Nevada.

Bubble Penetration Through a Single Layer Sphere Bed

Robert E. Manning*

Purdue University, West Lafayette, IN, 47907-2015, USA

Steven H. Collicott†

Purdue University, West Lafayette, IN, 47907-2015, USA

The stability criteria for a droplet passing through a tightly packed sphere monolayer are computed numerically. The Surface Evolver software is programmed to compute droplet shape and the corresponding stability properties under the influence of gravity. Sphere configurations from square to near hexagonal packing angles are considered. For a fixed volume and liquid contact angle, regions of stability are determined for a range of packing angles and Bond numbers. Furthermore due to the droplet forming contact lines with spheres, seven droplet topologies are compared to determine the lowest energy solution. This work compliments existing literature of a liquid infiltrating a sphere layer.

I. Introduction

Historically, hollow cylinders, uniform slits between plates, parallel rods, and toroidal pores [1] have been used as sample structures to model capillary phenomena in porous media. While these approaches have had various levels of success, a simple but very effective model is a set of uniformly close-packed solid spheres [1]. This structure can have various void fractions or porosities by changing the packing configuration. A cubic packed configuration ($\delta = 90^o$) has the maximum porosity at approximately 48%, while hexagonal packing ($\delta = 60^o$) is a minimum.

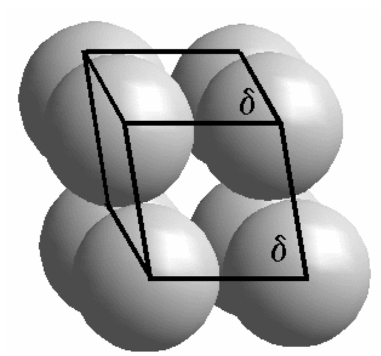

Figure 1. Three dimensionally packed spheres bed

This spherical structure, as seen in Figure 1, has been used extensively in infiltration problems. Using this model, Mayer and Stowe analytically derived expressions for capillary pressure. Hilden and Trumble numerically computed interface surfaces for a hexagonal-packed sphere layer with no gravity [2]. Extending

*Graduate Student, School of Aeronautics and Astronautics.

†Associate Professor, School of Aeronautics and Astronautics, 1375 Aviation Drive, and Associate Fellow.

their work, Slobozhanin, Alexander, Collicott, and Gonzalez incorporated gravity effects with both square and hexagonal-packed sphere layers [3].

An interesting but unexplored compliment of the infiltration problem is a liquid droplet passing through a sphere layer. This is of interest for a variety of applications, in particular inkjet-printing. Printing resolution is based on an understanding of pigment spreading on porous or fibrous media, such as paper [4].

Using a similar approach to Hilden-Trumbles work, the interface shape can be solved exactly. The criteria for droplet penetration and detachment is determined. Stable interfaces are categorized according to contact line formation. Furthermore, the solution presented is also valid for a gas bubble passing through a liquid filled pore.

II. Problem Formulation

We examine a single liquid droplet above a pore under the influence of gravity. The pore is formed by four solid spheres of radius r in a packed coplanar configuration (see Figure 2), ranging from square ($\delta = 90^o$) to hexagonal ($\delta = 60^o$) packing. The centers of the four spheres form a horizontal plane, which is normal to the ζ axis. The throat area of the pore is at a maximum when square and at a minimum when hexagonally packed. A liquid droplet that is placed above the pore has a volume ν and density ρ, as seen in Figure 3. It also has a prescribed surface tension γ and fixed contact angle θ. A stable droplet can impinge on one or more spheres. A uniform gravitational acceleration, g, is applied to the droplet. A positive acceleration pulls the droplet upward along the positive ζ axis.

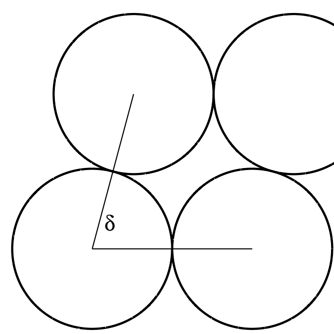

Figure 2. A single sphere layer with an arbitrary packing angle

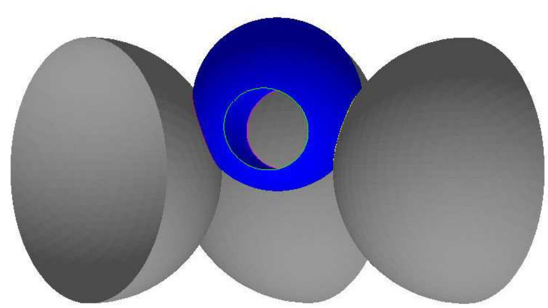

Figure 3. A four contact line solution from Surface Evolver with fourth sphere removed

The droplet progression through the pore is assumed to be quasi-static. This implies that the droplet is stable only if a static equilibrium exists. We model the droplet by minimizing the capillary and gravitational energies. The capillary pressure (Δp) is a function of surface tension γ and mean curvature H, as see in equation 1.

$$\Delta P = \frac{1}{2}\gamma H \tag{1}$$

The curvature H is defined as $\frac{1}{2}(k_1 + k_2)$ where k_1 and k_2 are the principle curvatures at each point on the capillary surface. Furthermore, for the fluid interface to be static, the hydrostatic pressure must balance the capillary pressure. The solid sphere radius is introduced as the characteristic length and results in the following dimensionless parameters:

$$B_o = \frac{\Delta \rho g r^2}{\gamma} \; Z = \frac{\zeta}{r} \; V = \frac{\nu}{r^3} \tag{2}$$

This introduces the Bond number, B_o, the ratio of gravitational energy to surface tension. The nondimensional volume V is scaled with the radius of the solid spheres r. Four different parameters uniquely determine the interface shape: packing angle δ, dimensionless droplet volume V, Bond number B_o, and contact angle θ.

III. Method of Solution

Due to the complexity of geometry, the three-dimensional interface surface is solved numerically using the Surface Evolver package. This interactive software program, developed by K.A. Brakke, computes surfaces described by a minimal energy functional and bound by various constraints. The surface is modeled as a union of triangles and is solved for using a gradient descent method [5]. In addition to solving for capillary surface equilibria, Surface Evolver is able to determine stability [3]. The dimensionless energy functional for a droplet under the influence of gravity is equation 3. Note that the area of the dry surface is neglected because the area of the rigid spheres is the same for all cases. This offsets all energies by a fixed amount, which can be ignored.

$$\frac{E}{\sigma r^2} = B_o \int z dV + S_{free} - cos\theta S_{wetted} \tag{3}$$

When examining the energy functional and geometry, we can determine several symmetries to reduce the complexity of the problem. First the geometry has no preferred direction in the Z axis. This implies that for every solution that is below the pore, there exists a corresponding solution above the sphere layer. Furthermore, the energy functional has the same form when both the Bond number and vertical distance to the center of mass change signs. Consequently, only solutions above the pore are required and can be used to generate the solutions below the pore by changing the signs of the Bond number and vertical distance to the center of mass (COM). Physically, the droplet, which is above the pore, is pushed into or pulled away from the pore for negative and positive Bond numbers, respectively.

Using a similar argument, a wetting gas bubble and non-wetting liquid droplet have the same interface shape and stability properties. The bubble solution can be obtained by taking the supplement of the gas-liquid contact angle and changing the direction of gravity. See reference six for details.

While Surface Evolver is quite flexible, it is unable to change topologies dynamically, e.g. four to three contact lines. This would then require fifteen cases to compute. However due to the two planes of symmetry, only seven are needed: 1 four-contact line case, 2 three-contact line cases, 3 two-contact line cases, and 1 one-contact line case. Figure 4 outlines and establishes nomenclature for the two and three contact line cases. The first digit refers to the number of contact lines formed, while the letter refers to the unique topology with ranking according to stability. For example, 2A refers to the droplet that forms contact lines with two adjacent spheres. A droplet that impinges on the two most distant spheres is least stable and is called 2C.

Lastly, we establish a necessary criterion for topologies with one or two contact lines. With no gravity, a droplet solution can take on an infinite number of positions for two contact lines or less. From this condition, it is inferred that an infinitesimally small negative bond number will force the droplet into the pore. However this will cause droplet to impinge on the other spheres and no longer have only two contact lines. This then implies that the smallest stable Bond number is equal to or greater than zero for one and two contact line topologies.

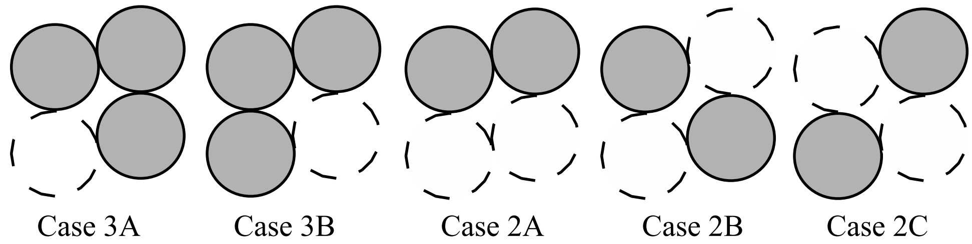

Figure 4. A list of identifiers is established for two and three contact lines cases. If the droplet has a contact line on a sphere, the sphere is gray.

A. Results

A set of stability regions for a droplet above the pore is calculated for unity volume and a liquid droplet contact angle of 135 degrees. The stable regions for each topology are plotted in three different figures. Cases 4, 2A, and 1 are plotted in Figure 5 for square to near hexagonal packing ($\delta = 65^o$). Note that 2A and 1 are not filled regions and are stable for $0 < B_o < 0.6$ and $0 < B_o < 0.5$, respectively. The stability boundaries for case 3A and 2B are dashed lines in this plot. Figure 6 displays cases 3A, 2A, 2B, and 1. The dashed lines in this figure outline case 4. Since topologies 3B and 2C are only possible for nearly square packings, Figure 7 focuses on $83^o < \delta < 90^o$. Once again, the inner dotted line references case 2B; while the outer one is case 3A. Note that 3A and 3B are the same shape at square packing. Results are accurate within 0.01 Bond number or greater, which is confirmed with two different stability tests that are outlined in Appendix A. Due to convergence difficulties with type 4 topologies, solutions for $60^o\delta < 65^o$ are not available.

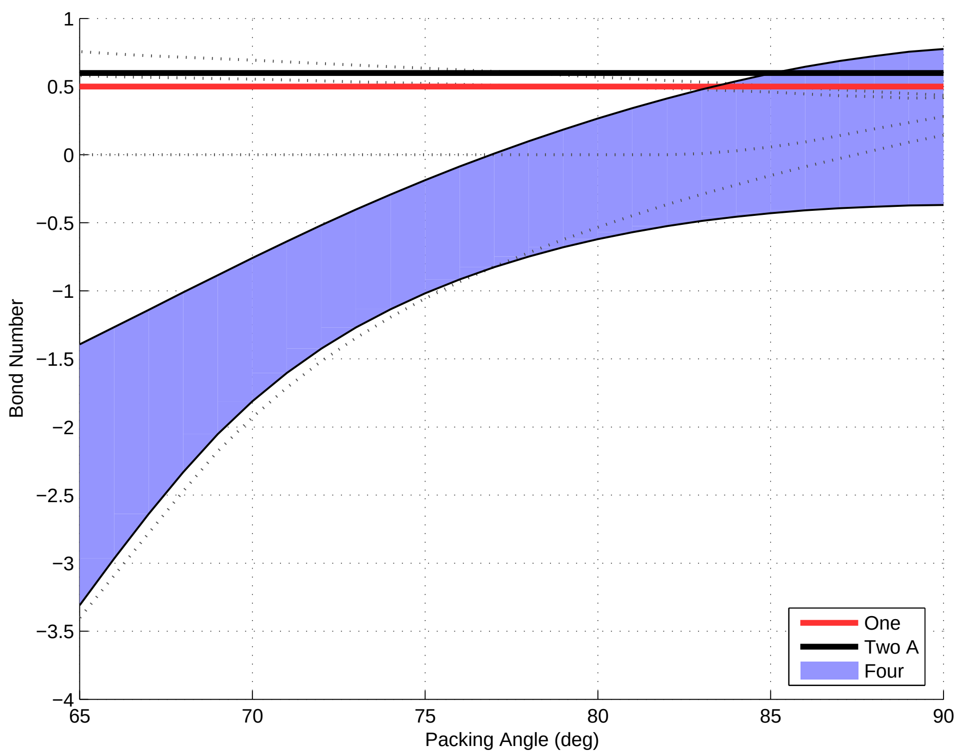

Figure 5. A stability plot for unity volume drop with 135 degree liquid contact angle.

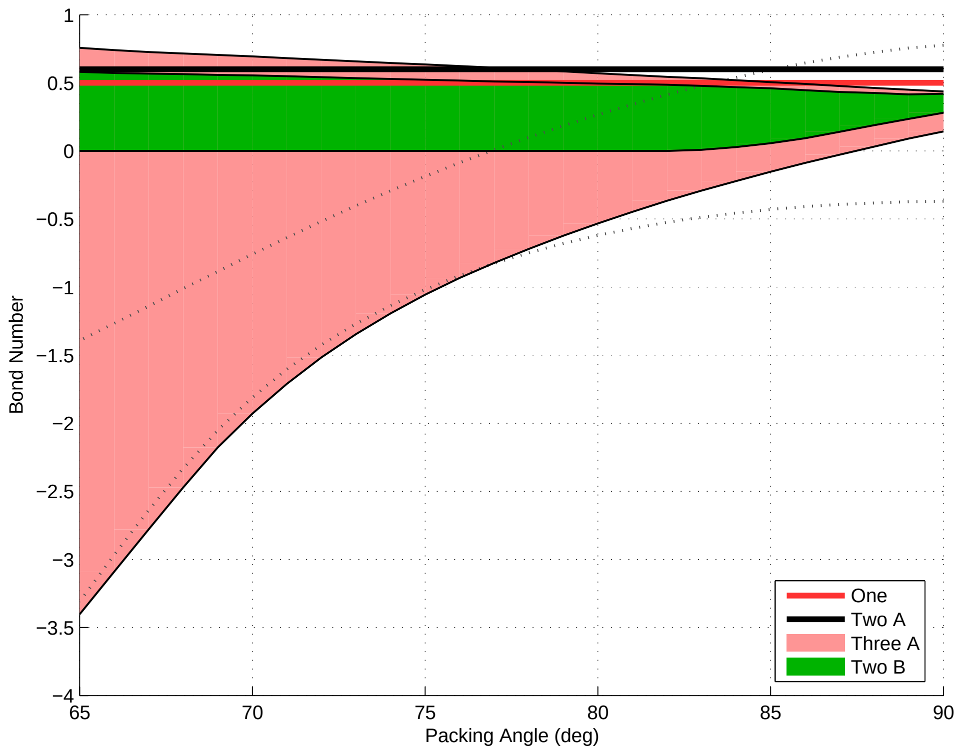

Figure 6. A stability plot for unity volume drop with 135 degree liquid contact angle.

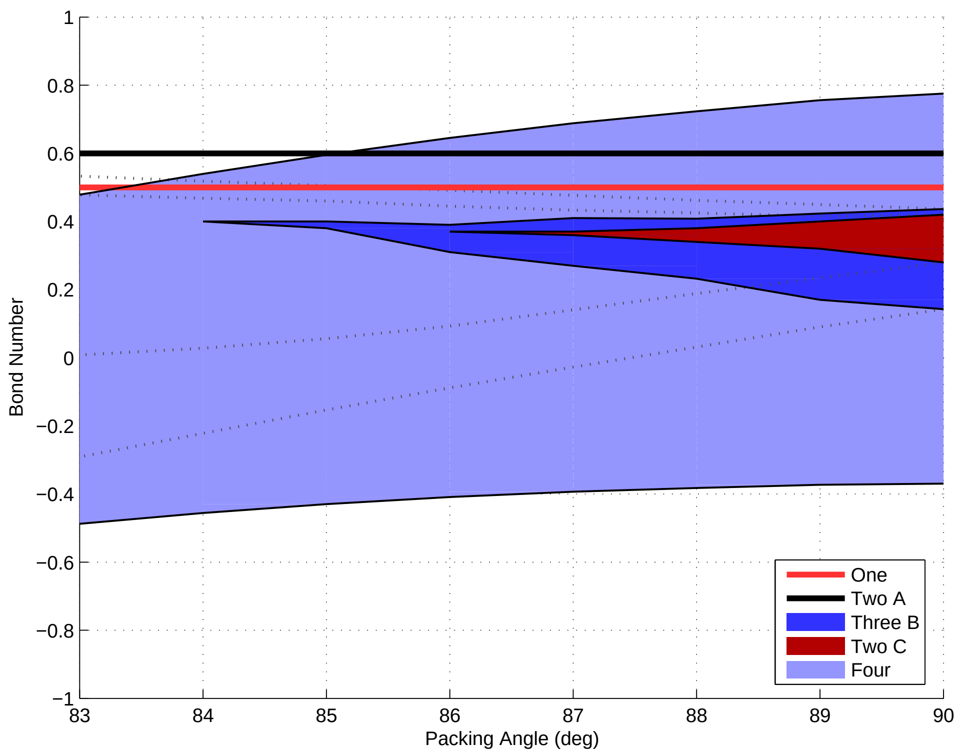

Figure 7. A stability plot for unity volume drop with 135 degree liquid contact angle, focusing on the near square packed geometries.

Using this quasi-static approach, we are able to establish some necessary conditions for stability of a droplet above the pore. (Consequently the criteria for a droplet below the pore are the same with a sign change of the Bond number and vertical location of the COM. However we will strictly consider the prior case for consistency.) When the Bond number exceeds an upper boundary of a topology, the topology will become unstable and may transition to another shape. However when the Bond number is greater than the largest stable Bond number, the droplet will drip and detach from the sphere layer. For packings $85^o < \delta < 90^o$, this drip boundary is the upper boundary of case 4 and is 0.78 Bond for square packing. For positive Bond numbers, an unstable type 1 or type 2A droplet cannot form contact lines. As a result, a droplet with one contact line will drip for $B_o > 0.5$ and a type 2A will do so for $B_o > 0.6$.

For packings between 78^o and 85^o, type 2A (droplet impinging on two adjacent spheres) is the only stable topology for $B_o = 0.6$. The droplet will then drip when the Bond number exceeds 0.6. Like before, type 1 droplets cannot transition to a more stable topology and will detach for $B_o > 0.5$. However, other topologies like case 4 and 3A may transition to 2A when instability occurs.

When the sphere layer is packed tighter than 78^o, then the upper boundary of 3A is the drip line. This topology has a larger stable region for positive Bond numbers than type 1 or 2A. As seen before, both case 1 and case 2A cannot transition to case 3A when $B_o > 0.5$ and $B_o > 0.6$, respectively. This behavior is also seen with type 2B when unstable. However a droplet with four contact lines can become 3A or others.

The lower (more negative Bond number) boundary is determined by the stability of case 4 and 3A. When the Bond number is less than this limit, the droplet will pass through the pore regardless of topology. For nearly square packing angles ($\delta > 83^o$), the droplet will pass through the pore for $-0.48 < B_o < -0.37$. However it may remain attached below the pore as a type 4, 3A, 2A, and 1 droplet. Also other topologies are possible as well for δ approximately greater than 86^o.

When δ is approximately 80^o, the droplet can pass through the pore when $B_o < -0.61$. However unlike near square packing configurations, the droplet does not remain attached to the bottom of the sphere layer. This occurs for $\delta < 80^o$ but at increasingly more negative Bond numbers due to the decreasing pore cross-sectional area. For $\delta < 77^o$, type 3A remains stable for more negative Bond numbers than type 4.

For a particular set of stable Bond number and packing angle, the liquid-gas interface can have single or multiple stable topologies. There are six regions where only one interface topology can exist. First for packing angles greater than 77^o, only a four contact line topology exists between the lower bounds of 3A and 4 cases. Between hexagonal packing and 77^o, the three contact line case is the only stable solution that is between the bounds for 4 and 2A and is below the lower bound for case 4. The fourth and fifth regions are type 4 for $\delta > 85^o$ and type 3A for $\delta < 78^o$ and are above the 2A upper stability limit. The sixth region is 2A and occurs between the fourth and fifth regions. In contrast, the 2C region, which only occurs when the sphere layer is closely square-packed, is stable for all other topologies.

B. Nearly square packed case

Using the results from the previous section, we will closely examine the droplet progression and pore passage for a droplet with a 135^o contact angle and unity volume. A packing angle of 88^o is chosen to illustrate all seven possible topologies. The vertical distance to the COM is plotted for all stable Bond numbers in Figure 8. Figure 9 focuses on a region of interest where 2B and 3C exist.

For the 88^o packing angle, we determine the static stability of a droplet for a range of Bond numbers. While this method is unable to determine the perturbation magnitude necessary to cause transition, it can determine possible resultant topologies and positions for a fixed Bond number. Also note that any transition due to instability can allow the droplet to take any stable topology or completely detach from the sphere layer. The result depends on the perturbation magnitude and droplet properties. The following discussion will disregard perturbations as a cause of transition.

For Bond numbers that force the droplet into the pore, the four contact line case is the only static equilibrium interface. As a result, a droplet may transition to type 4. When $Bo < -0.378$, the droplet cannot remain stable and will pass through the pore, as seen in Figure 8 at point B. If the magnitude of the Bond number is greater than 0.733, no stable solution exists on either side of the sphere layer.

The droplet can also transition to other topologies at various other Bond numbers. At point A in Figure 8, a 1 or 2A droplet will approach the sphere layer and form four contact lines. Another transition occurs at point C and D in Figure 9 where a 3-contact-line droplet will gain a fourth contact line. Also, at points E and F, a 2B and 2C topology will transition to a type 3A.

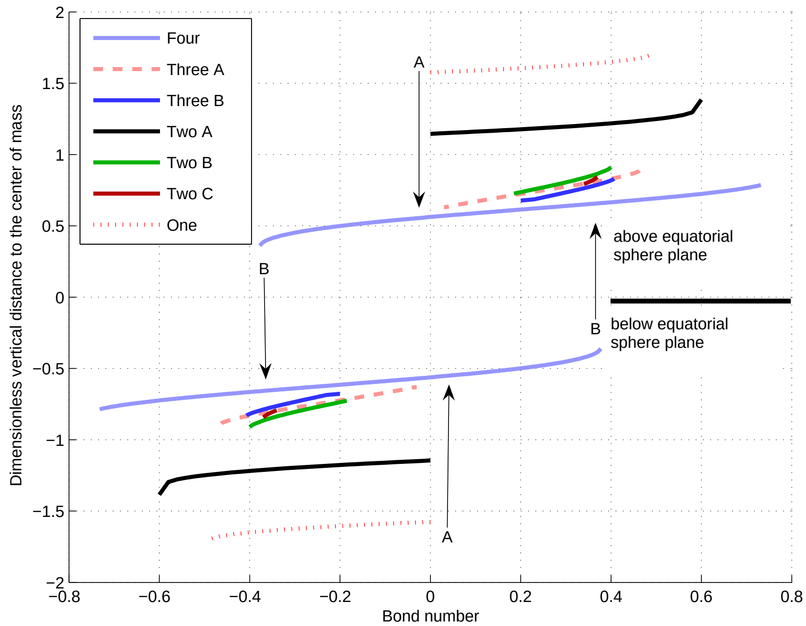

Figure 8. The center of mass of a unity volume droplet is solved for over a range of Bond numbers. The packing angle is 88 degrees.

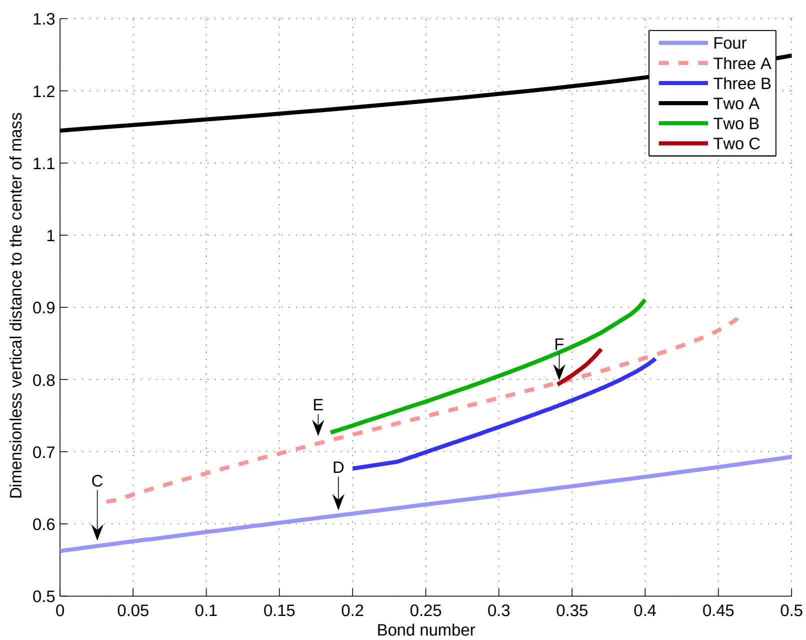

Figure 9. A detailed look at a region in the previous figure.

The vertical location of the COM is dependent on both the Bond number and the number of contact lines. For more negative Bond numbers, the droplet is pushed into the pore. Also the droplet is closer to the pore when it has more contact lines. In addition, the vertical distance to the COM of a stable interface can only lie in a particular set of ranges. For case 1, the vertical distance falls between 1.58 and 1.7. For case 2A, the range is 1.14 to 1.39. All other stable topologies will have a COM in $0.36 < z < 0.91$.

IV. Concluding Remarks

Using the Surface Evolver software package, static capillary surfaces were computed for a non-wetting (135^o) droplet passing through a sphere layer. For ranges of both packing angles and Bond numbers, the stability and shape of the droplet were analyzed. This analysis predicts a larger stable region for a droplet with two adjacent contact lines than for one with a single contact line. Criteria for droplet pore-passage were also established. The progression and center of mass of a droplet in a nearly square packed sphere layer were examined in detail. This work provides some preliminary analysis of sprays and droplet passage in porous media.

V. Acknowledgements

This work is supported in part by NASA research grant NNC05GA25G, Dr. Walter Duval, Program Manager. *Surface Evolver* was created by Professor K. A. Brakke of Susquehanna University and is available free at his web site, `http://www.susqu.edu/facstaff/b/brakke`.

VI. References

[1] R. P. Mayer and R. A. Stowe, Packed uniform sphere model for solids: Interstitial access opening sizes and pressure deficiencies for wetting liquids with comparison to reported experimental results, J. Colloid Interface Sci. 294, 139-150 (2006).

[2] J. L. Hilden and K. P. Trumble, Numerical analysis of capillarity in packed spheres: Planar hexagonal-packed spheres, J. Colloid Interface Sci. 267, 463-474 (2003).

[3] L. A. Slobozhanin, J. I. D. Alexander, S. H. Collicott, S. R. Gonzalez, Capillary pressure of a liquid in a layer of close-packed uniform spheres.

[4] R. K. Holman, M. J. Cima, S. A. Uhland, and E. Sachs, Spreading and infiltration of inkjet-printed polymer solution droplets on a porous substrate, J. Colloid Interface Sci. 249, 432-440 (2002).

[5] K. A. Brakke, Surface Evolver (manual and code), http://www.susqu.edu/facstaff/b/brakke.

[6] A. Myshkis, V. Babskii, N. Kopachevskii, L. A. Slobozhanin, and A. Tyuptsov, Zero-Gravity Fluid Mechanics: Mathematical Theory of Capillary Phonomena, Springer-Verlag, Berlin, 1990.

VII. Appendex A

Two different convergence tests were performed to determine the quantity of facets and iterations necessary to arrive at an accurate solution. The first test examined the energy and vertical distance to the center-of-mass (COM) over a variety of surface refinements. Two geometries were considered: a stable four contact-line case at square packing and a three contact-line droplet at 61^o packing angle. These surfaces were evolved until convergence for a range of facets: 200, 800, 1100, 3000, 8400, 15000, and 32000. The distance to the COM and energy were compared to the 32000-facet case. The COM distance and energy converged for higher levels of refinement.

Two additional cases with 32000 facets with 0.01 and 0.001 variations in Bond number were computed. When the interface is stable, the center-of-mass (COM) is relatively insensitive to small changes in Bond number; however, energy is quite sensitive. Approximately 3000 or greater number of facets is needed to accurately resolve variations of 0.01 Bond number. For thousandths accuracy, approximately 15000 facets are needed.

In addition to resolving changes in energy, Surface Evolver must also determine when the free surface impinges on any solid sphere. As in the previous test, the droplet has unity volume, a liquid contact angle of 135^o, and three contact lines. The sphere layer is near square packed with $\delta = 89^o$. The Bond number is increased in 0.001 increments until the interface touches the solid sphere. This procedure was done for several quantities of facets: 800, 1100, 3000, 8400, 15000, 32000, and the Bond number was recorded when the droplet impinged on the fourth sphere. For all cases, the Bond number does not vary more than 0.001. Thus, even a small number of facets can accurately determine when the free surface contacts a solid sphere.